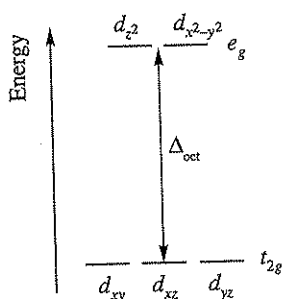


21 d-Block metal chemistry: coordination complexes

21.1 Refer to Section 21.3 in H&S. Points to include:

- Gas phase metal ion M^{n+} has degenerate nd atomic orbitals, and a valence configuration of nd^x .
- Consider formation of octahedral complex $[ML_6]^{n+}$. Crystal field theory treats metal ion and ligands as point charges; repulsions between electrons in M^{n+} d orbitals and L donor electrons.
- Ligands create a 'crystal field' around M^{n+} . In a spherical field, the energy of d orbitals is raised with respect to energy in gas phase M^{n+} . See left-hand side of Figure 21.2 in H&S.
- An octahedral crystal field leads to splitting of d orbitals into 2 sets (21.1): (i) higher energy d_{z^2} and $d_{x^2-y^2}$, and (ii) lower energy d_{xy} , d_{xz} and d_{yz} . The d_{z^2} and $d_{x^2-y^2}$ orbitals point *directly* at the ligands while d_{xy} , d_{xz} and d_{yz} orbitals point *between* the ligands. Therefore, repulsion between ligand electrons and electrons in d_{z^2} and $d_{x^2-y^2}$ is greater than between ligand electrons and electrons in d_{xy} , d_{xz} and d_{yz} orbitals. See right-hand side of Figure 21.2 in H&S.
- The raising and lowering of energies is measured with respect to the energy level in the spherical crystal field, this is the barycentre (see diagram 21.14).
- Include redrawn Figures 21.2 and 21.3 from H&S in your answer.

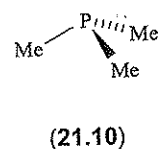
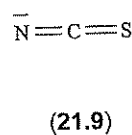
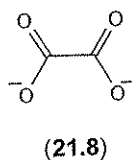
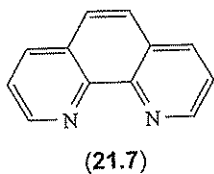
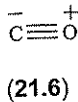
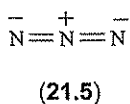
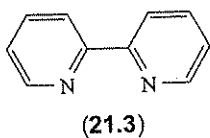
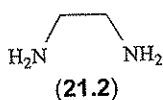


(21.1)

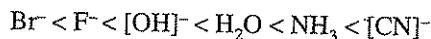
21.2 Look at Table 20.2 in H&S. λ_{\max} is the wavelength of the absorption maximum; a value of $\lambda_{\max} = 510$ nm corresponds to absorption of green light and transmittance of red and violet, so solutions of $[\text{Ti}(\text{H}_2\text{O})_6]^{3+}$ actually look purple.

- 21.3 (a) en = 1,2-ethanediamine; N,N' -donor, 21.2. Usually bidentate; forms 5-membered chelate ring (chelate effect, see Section 6.12 in H&S). Occasionally monodentate.
 (b) bpy = 2,2'-bipyridine; N,N' -donor, 21.3. Bidentate; 5-membered chelate ring.
 (c) Cyanide, $[\text{CN}]^-$ (21.4); usually C-donor, monodentate; sometimes bridges in an $\text{M}-\text{C}\equiv\text{N}-\text{M}$ mode (see examples in Chapter 22 of H&S).
 (d) Azide, $[\text{N}_3]^-$, (21.5); usually monodentate N-donor; sometimes bridges.
 (e) CO, (21.6); monodentate, C-donor (see Section 24.2 in H&S).
 (f) phen = 1,10-phenanthroline (21.7); N,N' -donor; bidentate forming 5-membered chelate ring.
 (g) $[\text{ox}]^{2-}$ = oxalate (21.8); O,O' -donor; bidentate forming 5-membered chelate ring.
 (h) $[\text{NCS}]^-$ (thiocyanate, 21.9) can be an N- or S-donor; usually monodentate but sometimes bridges in an $\text{M}-\text{N}=\text{C}=\text{S}-\text{M}$ mode.
 (i) PMe_3 (trimethylphosphine, 21.10) is usually a monodentate, P-donor, but see structure 24.18 in H&S and the accompanying discussion.

The order is as ligands appear in the spectrochemical series (Section 21.3 in H&S):



21.4



$\xrightarrow{\hspace{10em}}$
 weak field strong field

21.5 Factors to look for are different oxidation states of metal, different field strengths of ligands, or metals with same oxidation state and in the same triad.

(a) $[\text{Cr}(\text{OH}_2)_6]^{3+}$ should have larger Δ_{oct} than $[\text{Cr}(\text{OH}_2)_6]^{2+}$ (+3 is higher ox. state).

(b) $[\text{Cr}(\text{NH}_3)_6]^{3+}$ should have larger Δ_{oct} than $[\text{CrF}_6]^{3-}$ (both Cr(III), but NH_3 is a stronger field ligand than F^-).

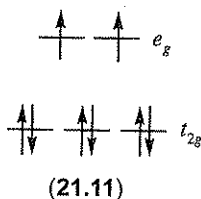
(c) $[\text{Fe}(\text{CN})_6]^{3-}$ is Fe(III), $[\text{Fe}(\text{CN})_6]^{4-}$ is Fe(II); $[\text{Fe}(\text{CN})_6]^{3-}$ will have larger Δ_{oct} .

(d) $[\text{Ni}(\text{en})_3]^{2+}$ should have larger Δ_{oct} than $[\text{Ni}(\text{OH}_2)_6]^{2+}$ (en is stronger field ligand).

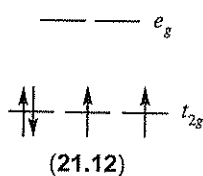
(e) $[\text{MnF}_6]^{2-}$ and $[\text{ReF}_6]^{2-}$ both contain M(IV) with M from group 7; $[\text{ReF}_6]^{2-}$ should have larger Δ_{oct} because Re is 3rd row metal, Mn is 1st row.

(f) $[\text{Co}(\text{en})_3]^{3+}$ and $[\text{Rh}(\text{en})_3]^{3+}$ both contain M(III) with M from group 9; $[\text{Rh}(\text{en})_3]^{3+}$ should have larger Δ_{oct} because Rh is 2nd row metal, Co is 1st row.

21.6 (a) Diagram 21.11 shows the d^8 configuration in an octahedral field. There is no vacant e_g orbital and so no possibility of promoting an electron from a fully occupied t_{2g} orbital to generate a high-spin configuration. \therefore Only one configuration.

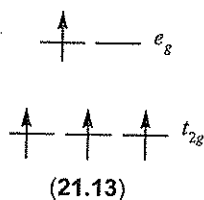


(b) Consider an example, e.g. octahedral d^4 , that can be low-spin (21.12) or high-spin (21.13). Preference for high-spin or low-spin configuration depends on which configuration has the lower energy. This, in turn, depends on whether it is energetically preferable to pair the fourth electron (21.12) or promote it to the e_g level (21.13). Need to consider the energy required to transform two electrons with parallel spins in different degenerate orbitals into spin-paired electrons in the same orbital – the pairing energy, P , depends on (i) the loss in the *exchange energy* on pairing the electrons (see Box 1.8 in H&S), and (ii) the coulombic repulsion between the spin-paired electrons.



For high-spin: $\Delta_{\text{oct}} < P$ weak field
 For low-spin: $\Delta_{\text{oct}} > P$ strong field

(c) Different numbers of unpaired electrons give rise to different effective magnetic moments (μ_{eff}), e.g. low-spin d^4 has 2 unpaired electrons, high-spin d^4 has 4. Use the spin-only formula to estimate the magnetic moment for n unpaired electrons:



$$\mu_{\text{spin-only}} = \sqrt{n(n+2)}$$

In the case of an octahedral d^6 ion, low-spin is diamagnetic, high-spin is paramagnetic.

21.7 For a given d^n configuration, CFSE is *difference* in energy between d electrons in octahedral crystal field and d electrons in spherical crystal field. From diagram 21.14:

$$\text{CFSE} = (-0.4\Delta_{\text{oct}})(\text{number of electrons in } t_{2g} \text{ level}) + (0.6\Delta_{\text{oct}})(\text{number of electrons in } e_g \text{ level})$$

Examples of use of this equation:

$$\begin{aligned} d^1 & \text{ CFSE} = (-0.4\Delta_{\text{oct}})(1) + 0 = -0.4\Delta_{\text{oct}} \\ d^4 \text{ high-spin} & \text{ CFSE} = (-0.4\Delta_{\text{oct}})(3) + (0.6\Delta_{\text{oct}})(1) = -0.6\Delta_{\text{oct}} \\ d^5 \text{ high-spin} & \text{ CFSE} = (-0.4\Delta_{\text{oct}})(3) + (0.6\Delta_{\text{oct}})(2) = 0 \end{aligned}$$

But for, for example, low-spin d^4 , CFSE consists of two terms: the four electrons in the t_{2g} orbital give rise to a $-1.6\Delta_{\text{oct}}$ term and a pairing energy, P , must be included to account for the spin-pairing of two electrons:

$$\text{CFSE} = -1.6\Delta_{\text{oct}} + P$$

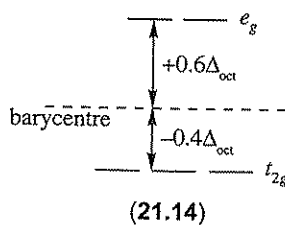
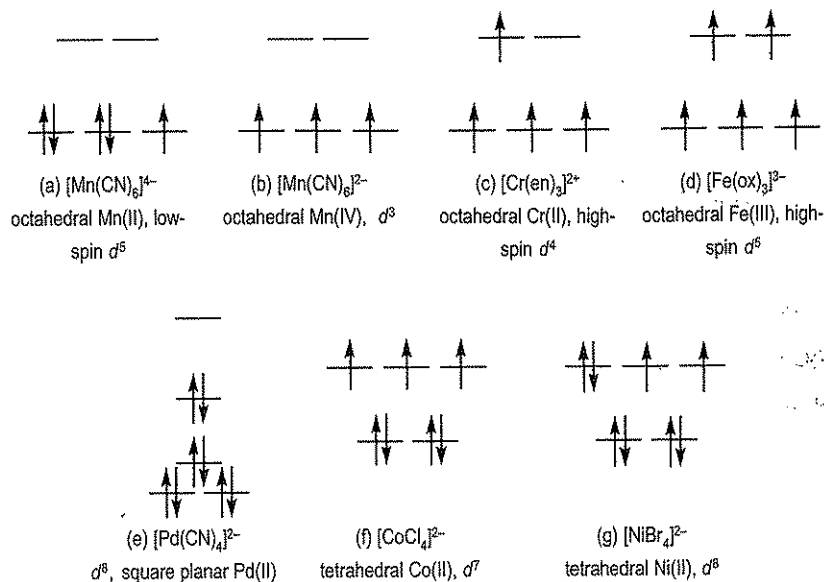
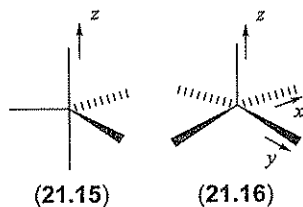


Figure 21.1 For answer 21.8: rationalizing numbers of unpaired electrons in problem 21.8. For the ground state electronic configurations of the metal atoms, see Table 20.1, p. 256.



21.8 See Figure 21.1.

21.9 (a) Define an axis set; by convention, take the axial ligands to lie on the z axis (21.15 and 21.16).



Trigonal bipyramid: the d_{z^2} orbital points directly at 2 ligands and is destabilized the most (Figure 21.2). The equatorial ligands lie in the xy plane, and the $d_{x^2-y^2}$ and d_{xy} orbitals are degenerate and higher in energy than the d_{xz} and d_{yz} orbitals which point between the ligands. **Square-based pyramid:** 1 ligand lies on the z axis, 2 lie \approx along the x axis, 2 lie \approx on the y axis; the $d_{x^2-y^2}$ orbital (points \approx at the basal ligands) is destabilized the most, the d_{z^2} orbital is destabilized to a lesser extent (Figure 21.2); since the basal ligands lie in the xy plane, the d_{xy} orbital lies at higher energy than the d_{xz} and d_{yz} orbitals.

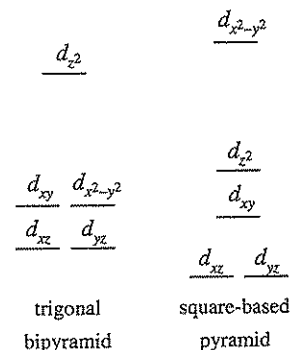
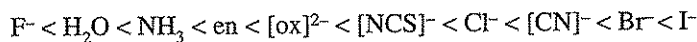


Figure 21.2 For answer 21.9: crystal field splitting diagrams for trigonal bipyramidal and square-based pyramidal fields.

(b) Ni(II) is d^8 and both trigonal bipyramidal and square-based pyramidal complexes will be diamagnetic (place 8 electrons in the levels shown in Figure 21.2).

21.10 (a) On going from gaseous M^{n+} to complexed M^{n+} , interelectronic repulsion between metal d electrons decreases – pairing energies reduced. This is caused by an increase in effective size of metal orbitals – the *nephelauxetic effect* ('cloud expanding'). For a common M^{n+} , nephelauxetic effect of ligands follows series:



For metal ions (with a common ligand) nephelauxetic effect follows series:



Parameters for ligands (h) and metal ions (k) (see Table 21.10 in H&S) are used to estimate the reduction in electron-electron repulsion upon complex formation:

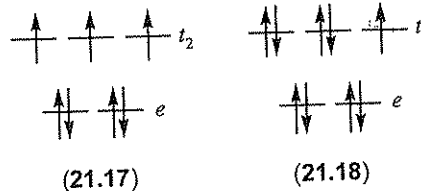
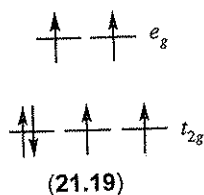
$$\frac{B_0 - B}{B_0} \approx (h_{\text{ligands}})(k_{\text{metal ion}})$$

where B is the Racah parameter, B_0 is interelectronic repulsion in free ion.

(b) From nephelauxetic series for ligands: $F^- < H_2O < NH_3 < en < [CN]^- < I^-$

21.11 (a) $[CoCl_4]^{2-}$ is Co(II), d^7 . $[CuCl_4]^{2-}$ is Cu(II), d^9 .

Tetrahedral Co^{2+} (21.17), t_2 orbitals are all singly occupied; in tetrahedral Cu^{2+} (21.18), t_2 orbitals are asymmetrically filled. Thus, the complex suffers a Jahn-Teller distortion leading to the observed flattened tetrahedron.



(b) Octahedral $[CoF_6]^{3-}$ is Co(III), d^6 . F^- is weak field ligand; ground state is high-spin (21.19). A d^6 ion might be expected to give a single absorption in the electronic spectrum (see diagram in Figure 21.19 in H&S). The excited state of $[CoF_6]^{3-}$ ($t_{2g}^3 e_g^3$) suffers a Jahn-Teller effect because the e_g level is asymmetrically filled. Small splitting of e_g level leads to 2 possible transitions: 11500 and 14500 cm^{-1} .

21.12 The electron configuration of Si is $1s^2 2s^2 2p^6 3s^2 3p^2$, but only the $3p^2$ ($l = 1$) configuration contributes to the term symbol. The working is as for carbon in Section 21.6 in H&S. There are 15 microstates. The table of microstates for a p^2 configuration is given in Table 21.6 in H&S. The microstates are grouped according to values of M_L and M_S . Values of L and S are derived by looking for sets of M_L and M_S values:

$$\begin{aligned} \text{allowed values of } M_L: & L, (L-1), \dots, 0, \dots, -(L-1), -L \\ \text{allowed values of } M_S: & S, (S-1), \dots, -(S-1), -S \end{aligned}$$

Term symbols are assigned as follows:

- $L = 2, S = 0$ gives the singlet term, 1D ; J can take values $(L+S), (L+S-1), \dots, |L-S|$, so only $J = 2$ is possible; the term symbol is 1D_2 .
- $L = 1, S = 1$ corresponds to a doublet term; possible values of J are 2, 1, 0 giving the terms $^3P_2, ^3P_1$ and 3P_0 .
- $L = 0, S = 0$ corresponds to a singlet term, and only $J = 0$ is possible; the term symbol is 1S_0 .

The predicted energy ordering (from the rules above) is $^3P_0 < ^3P_1 < ^3P_2 < ^1D_2 < ^1S_0$.

21.13 3F and 3P are triplet terms. $^1D, ^1G$ and 1S are singlet terms. Electronic transitions obey the spin selection rule:

$$\Delta S = 0$$

i.e. transitions may occur from singlet to singlet, or triplet to triplet states, but a change in spin multiplicity is forbidden.

The relative energies of the $^3F, ^3P, ^1D, ^1G$ and 1S terms are determined using Hund's rules. The terms with the highest spin multiplicity are the 3F and 3P , and of these, the term with higher value of L has the lower energy. Therefore, 3F is the ground term. The other terms are singlets and their relative energies depend on the values

of L . The energy ordering of the terms for a d^2 configuration is therefore ${}^3F < {}^3P < {}^1G < {}^1D < {}^1S$. The most probable transitions originate from the ground state. The allowed transition (triplet to triplet in an absorption spectrum) is ${}^3F \leftarrow {}^3P$. Transition from ground to excited states are much more likely than from excited to excited states, and therefore you can ignore the latter on statistical grounds.

21.14 d^{10} is a closed shell configuration and gives only a 1S term. For this term, $L = 0$, $S = 0$, and therefore $J = 0$. Using the following formula:

$$\text{Multiplicity of the term} \longrightarrow (2S+1)L_J \longleftarrow \begin{matrix} S, P, D, F, G \dots \text{ term} \\ J \text{ value} \end{matrix}$$

the ground (and only) term is therefore 1S_0 . Examples of d^{10} ions: Zn^{2+} , Cu^+ .

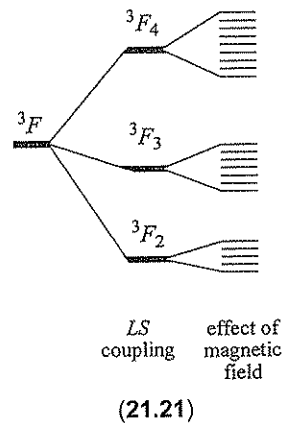
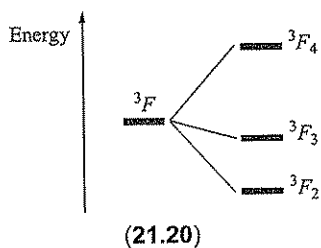
21.15 Russell-Saunders coupling is a spin-orbit coupling scheme and it is not valid for all elements, in particular those with high atomic numbers. For heavier elements where spin-orbit coupling is particularly large, a more appropriate approach is to use a jj -coupling scheme.

For detailed discussions, see:

T.P. Softley (1994) *Atomic Spectra*, Oxford University Press, p. 68;

M. Gerloch (1986) *Orbitals, Terms and States*, Wiley, p. 73.

21.16 The quantum number J takes values $(L+S)$, $(L+S-1) \dots |L-S|$. For the 3F term, $L = 3$ and $S = 1$. Therefore, $J = 4, 3, 2$. Different values of J denote different levels within the term (diagram 21.20), and the energy differences between successive pairs of energy levels are 3λ and 4λ where λ is the spin-orbit coupling constant. The degeneracy of a J level is $(2J+1)$. For $J = 4$, degeneracy = 9; for $J = 3$, degeneracy = 7; for $J = 2$, degeneracy = 5. In a magnetic field, each J state splits into the $(2J+1)$ levels separated by $g_J \mu_B B_0$ (g_J is the Landé g -factor, μ_B is the Bohr magneton, and B_0 is the magnetic field). The splitting of the levels in a magnetic field (shown in diagram 21.21) is called the Zeeman electronic effect, and the small energy separations between these levels are the basis for electron paramagnetic resonance (EPR) spectroscopy (see Box 20.1 in H&S).



Term

Components in octahedral field

S

A_{1g}

P

T_{1g}

D

$E_g + T_{2g}$

F

$A_{2g} + T_{2g} + T_{1g}$

G

$A_{1g} + E_g + T_{2g} + T_{1g}$

21.17 The splitting of terms in an octahedral field is tabulated in the margin.

(a) The 2D term will split to ${}^2T_{2g}$ and 2E_g .

(b) The 3P term does not split but becomes the ${}^3T_{1g}$.

(c) The 3F term splits to become the ${}^3T_{1g}$, ${}^3T_{2g}$ and ${}^3A_{2g}$.

See Figure 21.20 in H&S.

Table 21.1 Table of microstates for a d^1 ion.

m_l	-2				↑	
	-1				↑	
	0			↑		
	+1		↑			
	+2	↑				
M_L		+2	+1	0	-1	-2
		2D				

Table 21.2 Table of microstates for a d^2 ion.

m_l	-2				↑	↑	↑	↑	
	-1				↑	↑	↑	↑	
	0				↑	↑	↑	↑	
	+1		↑					↑	
	+2	↑	↑	↑	↑				
M_L		+3	+2	+1	0	-1	-2	-3	
		3F						3P	

- 21.18 The construction of tables of microstates is described in detail in Section 21.6 in H&S. Assume for this answer that you need only consider the *weak field limit*, i.e. terms of maximum spin multiplicity (see discussion in H&S, Section 21.6). Set up the table of microstates as in Table 21.1. The left-hand column in the top part of Table 21.1 gives m_l values for a d orbital; the row in the lower part of Table 21.1 gives M_L values for a d^1 ion. In a tetrahedral field, the 2D term has E and T_2 components (see Orgel diagram in Figure 21.19 in H&S). The multiplicity of the term (the 2 in the 2D symbol) is determined from $2S + 1$; for 1 electron, $S = 1/2$.
- (b) Set up the table of microstates for the d^2 ion remembering that the electrons singly occupy orbitals (Table 21.2). The M_L values are obtained by summing the m_l values in each column. Your table may not look identical to Table 21.2 because the columns may come in a different order; the columns here are arranged to give the values of M_L in an order from which the term symbols are easily found. The 3P term does not split (see answer 21.17) and gives a T_1 component in a tetrahedral field, and a T_{1g} component in an octahedral field. In an octahedral field, the components of the 3F term are A_{2g} , T_{2g} and T_{1g} ; in a tetrahedral field, they are A_2 , T_2 and T_1 .

- 21.19 (a) Equations needed:

$$\text{Wavenumber (in cm}^{-1}\text{)} = \frac{1}{\text{Wavelength (in cm)}} \quad 1 \text{ cm} = 10^7 \text{ nm}$$

► **Remember:** lower wavenumber corresponds to longer wavelength

► Visible range of spectrum and absorption/transmittance of light: see Table 20.2 in H&S

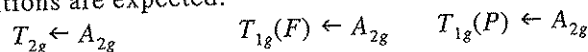
$$10\,000 \text{ cm}^{-1} = 1000 \text{ nm}; \quad 20\,000 \text{ cm}^{-1} = 500 \text{ nm}; \quad 30\,000 \text{ cm}^{-1} = 333 \text{ nm}.$$

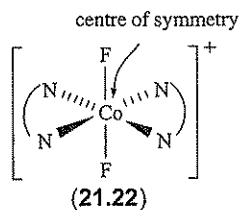
(b) Visible range $\approx 400\text{--}750 \text{ nm}$ ($25\,000\text{--}14\,285 \text{ cm}^{-1}$).

(c) Look at λ corresponding to the visible part of spectrum. $[\text{Ni}(\text{OH}_2)_6]^{2+}$ absorbs $\approx 660 \text{ nm}$, so appears green; $[\text{Ni}(\text{NH}_3)_6]^{2+}$ absorbs $\approx 570 \text{ nm}$, so appears purple.

(d) Consider positions of NH_3 and H_2O in spectrochemical series: H_2O is a weaker field ligand than NH_3 . The relative energies of transitions are estimated from an Orgel diagram (Figure 21.20 in H&S) and for the weaker field ligand, the transition energies are lower, i.e. $[\text{Ni}(\text{OH}_2)_6]^{2+} < [\text{Ni}(\text{NH}_3)_6]^{2+}$. Since E is proportional to wavenumber, the absorptions for $[\text{Ni}(\text{OH}_2)_6]^{2+}$ appear at lower wavenumbers than those for $[\text{Ni}(\text{NH}_3)_6]^{2+}$.

- 21.20 (a) Cr(III) is d^3 . Sketch an Orgel diagram for an octahedral d^3 ion. This corresponds to the left-hand side of Figure 21.20 in H&S. Three absorption transitions are expected:





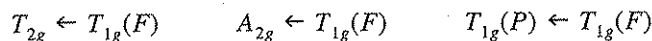
(b) *trans*-[Co(en)₂F₂]⁺ (21.22) has a centre of symmetry, but the *cis*-isomer does not; loss of centre of symmetry permits greater *p-d* mixing and, therefore, a greater probability of transitions, leading to more intense colour for the *cis*-isomer. Comparing chloro and fluoro *trans*-complexes: charge transfer from Cl⁻ to Co³⁺ (LMCT) accounts for the more intense colour of chloro complex; LMCT for F⁻ is unlikely. LMCT occurs when a ligand that is easily oxidized is bound to a metal centre (usually one in a high oxidation state) that is readily reduced.

21.21 (a) LMCT bands are at 282 nm for [OsCl₆]³⁻ and at 348 nm for [RuCl₆]³⁻. The LMCT band moves to longer wavelength (smaller energy) because it is easier to reduce Ru(III) than Os(III).

(b) The bpy ligand easily accepts an electron and therefore charge transfer will be in the direction M(II) to L, not L to M(II), i.e. an MLCT band rather than an LMCT band is observed.

21.22 [Ti(OH₂)₆]³⁺ is a *d*¹ ion. Its electronic spectrum consists of two bands close together (observed as one band with a shoulder) because of a Jahn-Teller effect in the excited state, *t*_{2g}⁰*e*_g¹. Single occupancy of the *e*_g level lowers the degeneracy, but the energy separation between the *t*_{2g} and *e*_g levels is small. Two '*d-d*' transitions from ground to excited state are therefore possible, but they are close in energy and give rise to absorptions at similar wavelengths.

[Ti(OH₂)₆]²⁺ is a *d*² ion. Three '*d-d*' transitions are predicted (Figure 21.20 in H&S):



but only two, well separated bands are observed in the absorption spectrum (see answer 21.38b).

21.23 Figure 21.23b in H&S shows the ⁴*F* and ⁴*P* terms arising from a *d*³ configuration. There are three transitions and their energies, measured from the electronic spectrum, are given by:

$$\begin{aligned} {}^4T_{2g} &\leftarrow {}^4A_{2g} & E &= \Delta_{\text{oct}} \\ {}^4T_{1g}(F) &\leftarrow {}^4A_{2g} & E &= 1.8\Delta_{\text{oct}} - x \\ {}^4T_{1g}(P) &\leftarrow {}^4A_{2g} & E &= 1.2\Delta_{\text{oct}} + 15B + x \end{aligned}$$

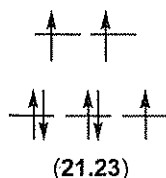
Limitations:

(i) The figure refers only to the extreme weak field limit and this is a severe limitation of the method outlined here for determining the Racah parameter *B*.

(ii) The method is easiest to apply if all three transitions are observed. If only two bands are observed (e.g. one absorption is hidden under an intense charge transfer band), it becomes more difficult to abstract a value for *B* from the observed data.

See: A.B.P. Lever (1968) *J. Chem. Educ.*, vol. 45, p. 711

21.24 (a) Co(II) is *d*⁷, and the Orgel diagram for octahedral *d*⁷ is the same as for octahedral *d*² (Figure 21.20 in H&S). Absorption data in the question are reported in cm⁻¹, and the smallest wavenumber corresponds to the lowest energy transition. H₂O is a mid-field ligand; an assumption has to be made about the crossing of the lines in the Orgel diagram. [Co(OH₂)₆]²⁺ is high-spin (21.23) with 3 unpaired electrons:



$$\text{Multiplicity} = (2 \times 3/2) + 1 = 4$$

The assignments are:

$$\begin{aligned} 8100 \text{ cm}^{-1} & \quad 4T_{2g} \leftarrow 4T_{1g}(F) \\ 16000 \text{ cm}^{-1} & \quad 4T_{1g}(P) \leftarrow 4T_{1g}(F) \\ 19400 \text{ cm}^{-1} & \quad 4A_{2g} \leftarrow 4T_{1g}(F) \end{aligned}$$

(b) From Figure 21.23a in H&S:

$$0.8\Delta_{\text{oct}} + x = 8100 \text{ cm}^{-1} \quad (\text{i})$$

$$1.8\Delta_{\text{oct}} + x = 16000 \text{ cm}^{-1} \quad (\text{ii})$$

Equation (ii) – (i) gives:

$$\Delta_{\text{oct}} = 16000 - 8100 = 7900 \text{ cm}^{-1}$$

This value does not agree with the value listed in Table 21.2 because the method is applicable only to a limiting case where field strength of the ligands is extremely weak.

21.25 Racah parameters provide information about electron–electron repulsions. On going from a gaseous metal ion to a metal complex, there is an effective expansion of ‘metal’ orbitals associated with metal–ligand bond formation. This results in a reduction in the electron–electron repulsions and, therefore, a reduction in the Racah parameter *B*. Parameters for ligands and metal ions (see answer 21.10a, p. 267) may be used to estimate this reduction.

21.26 Use the spin-only formula to find the number of unpaired electrons, or fit values calculated from the spin-only formula to the experimental values (assume you can ignore contribution of the orbital angular momentum to the magnetic moment):

Table 21.3 Calculated values of $\mu(\text{spin-only})$ for *n* unpaired electrons.

<i>n</i>	$\mu(\text{spin-only}) / \mu_{\text{B}}$
1	1.73
2	2.83
3	3.87
4	4.90
5	5.92

$$\mu(\text{spin-only}) = \sqrt{n(n+2)}$$

From values in Table 21.3:

(a) $[\text{VCl}_x(\text{bpy})]$ has 1 unpaired electron; d^1 corresponds to V(IV), therefore $x = 4$.

(b) $\text{K}_x[\text{V}(\text{ox})_3]$ has 2 unpaired electrons; d^2 corresponds to V(III); the complex anion is therefore $[\text{V}(\text{ox})_3]^{3-}$ and so $x = 3$.

(c) $[\text{Mn}(\text{CN})_6]^{x-}$ has 3 unpaired electrons; d^3 corresponds to Mn(IV); since the cyano ligand is $[\text{CN}]^-$, the overall charge must be $2-$, i.e. $x = 2$.

21.27 For an electron to have orbital angular momentum, it must be possible to transform the orbital containing the electron into an equivalent and degenerate orbital by rotation. For a fuller explanation, refer to Section 21.9 in H&S, the subsection entitled ‘Spin and orbital contributions to the magnetic moment’.

21.28 (a) $\text{K}_3[\text{TiF}_6]$ contains $[\text{TiF}_6]^{3-}$, therefore Ti(III), d^1 .

$$\mu(\text{spin-only}) = \sqrt{n(n+2)} = \sqrt{3} = 1.73 \mu_{\text{B}}$$

(b) In a d^1 ion (t_{2g}^1), there is one electron in one of the d_{xy} , d_{yz} or d_{zx} orbitals. These orbitals can be interconverted by rotations through 90° , and therefore the electron has orbital angular momentum. This results in an orbital contribution to the magnetic moment.

21.29 Octahedral Ni^{2+} (d^8) should have no orbital contribution, and μ_{eff} is expected to be close to spin-only value. Tetrahedral Ni^{2+} has an orbital contribution because ground state configuration is $e^4 t_2^4$, and so spin-orbit coupling occurs. This results in $\mu_{\text{eff}} > \mu(\text{spin-only})$. In a square planar Ni^{2+} complex, all electrons are paired leading to a diamagnetic complex; look at Figure 21.1e, p. 267 – the promotion energy to the d_z^2 orbital (highest level) is too large for a high-spin complex to form.

21.30 Consider for which ions you expect there to be an orbital contribution to the magnetic moment. Orbital contributions to the magnetic moment are important only for the t_{2g}^1 (see answers 21.28b and 21.35c), t_{2g}^2 , $t_{2g}^4 e_g^2$ and $t_{2g}^5 e_g^2$ configurations.

- | | | |
|-------------------------|--|-------------------------|
| (a) $[Cr(NH_3)_6]^{3+}$ | octahedral d^3 (t_{2g}^3) | no orbital contribution |
| (b) $[V(OH_2)_6]^{3+}$ | octahedral d^2 (t_{2g}^2) | orbital contribution |
| (c) $[CoF_6]^{3-}$ | octahedral, high-spin d^6 ($t_{2g}^4 e_g^2$) | orbital contribution |

Therefore, only for (a) will the spin-only formula give a reasonable estimate of the magnetic moment. An octahedral d^3 ion has a ${}^4A_{2g}$ ground term, and a better estimate of the magnetic moment can be obtained by using equation 21.23 in H&S.

21.31 All the examples in the question are octahedral complexes.

- | | |
|-------------------------|--|
| (a) $[Co(OH_2)_6]^{3+}$ | Co(III), low-spin d^6 , diamagnetic. |
| (b) $[CoF_6]^{3-}$ | Co(III), rare example of high-spin d^6 , paramagnetic. |
| (c) $[NiF_6]^{2-}$ | Ni(IV), low-spin d^6 , diamagnetic. |
| (d) $[Fe(CN)_6]^{3-}$ | Fe(III), strong-field ligand, low-spin d^5 , paramagnetic. |
| (e) $[Fe(CN)_6]^{4-}$ | Fe(II), strong-field ligand, low-spin d^6 , diamagnetic. |
| (f) $[Mn(OH_2)_6]^{2+}$ | Mn(II), high-spin d^5 , paramagnetic. |

21.32 (a) r_{ion} is estimated from ionic lattice; r_{ion} values for high-spin, octahedral ions are:

Ti ²⁺	V ²⁺	Cr ²⁺	Mn ²⁺	Fe ²⁺	Co ²⁺	Ni ²⁺	Cu ²⁺	Zn ²⁺
d^2	d^3	d^4	d^5	d^6	d^7	d^8	d^9	d^{10}
$t_{2g}^2 e_g^0$	$t_{2g}^3 e_g^0$	$t_{2g}^3 e_g^1$	$t_{2g}^3 e_g^2$	$t_{2g}^4 e_g^2$	$t_{2g}^5 e_g^2$	$t_{2g}^6 e_g^2$	$t_{2g}^6 e_g^3$	$t_{2g}^6 e_g^4$
86	79	80	83	78	75	69	73	74pm

Plot of r_{ion} against number of d electrons shows an 'inverse' double-humped curve. Radii increase at points in series when electrons enter d_z^2 or $d_{x^2-y^2}$ orbitals – these point directly at the ligands, and interelectronic repulsion increases.

(b) The trend is the inverse of that for lattice energies (Figure 21.33 in H&S). Lattice energy is inversely proportional to the internuclear separation and is therefore inversely related to r_{cation} . The double hump is rationalized in terms of variation in LFSE (include a graph or table of LFSE vs d^n electrons, Figure 22.32 in H&S). Hydration enthalpies (Figure 21.34 in H&S) behave similarly to lattice energies.

21.33 Normal spinel has tetrahedral Ni^{2+} (d^8) and 2 octahedral Mn^{3+} (d^4); inverse spinel has tetrahedral Mn^{3+} , octahedral Mn^{3+} and octahedral Ni^{2+} . One octahedral Mn^{3+} is

common to both types of spinel and can be neglected. Compare LFSE values:

$$\Delta_{\text{tet}} \approx 4/9 \Delta_{\text{oct}}$$

▶ LFSE tet. Ni^{2+} + oct. $\text{Mn}^{3+} = -(0.8 \times 4/9 \times 8500) - (0.6 \times 21\,000) = -15\,622 \text{ cm}^{-1}$
 ▶ LFSE oct. Ni^{2+} + tet. $\text{Mn}^{3+} = -(1.2 \times 8500) - (0.4 \times 4/9 \times 21\,000) = -13\,933 \text{ cm}^{-1}$

▶ Therefore, one predicts a normal spinel; the factor not taken into account is the Jahn-Teller effect for Mn^{3+} (d^4); although one predicts a normal spinel by a small margin, the structure is, in practice, an inverse spinel.

Spinel AB_2O_4 ; see Box 13.6 and Section 21.10 in H&S

21.34 (a) LFSEs can be estimated as in answer 21.7 – see also Table 21.3 in H&S. The difference in LFSE on going from octahedral $[\text{Co}(\text{OH}_2)_6]^{2+}$ to tetrahedral $[\text{CoCl}_4]^{2-}$ is much less for Co^{2+} (d^7) than for Ni^{2+} (d^8). Remember that $\Delta_{\text{tet}} \approx 4/9 \Delta_{\text{oct}}$.

▶ (b) Data are consistent with $\text{H}_4[\text{Fe}(\text{CN})_6]$ being a weak acid with respect to the 4th acid dissociation constant; H^+ complexing of $[\text{Fe}(\text{CN})_6]^{4-}$ makes reduction easier.

Refer to Section 8.3 in H&S

▶ (c) LFSE plays only a minor part. There is a loss of LFSE on reduction of Mn^{3+} (d^4), a gain on reduction of Fe^{3+} (d^5), and a loss on reduction of Cr^{3+} (d^3); the decisive factor is the large value of the 3rd ionization energy for Mn.

Refer to Section 21.12 in H&S

21.35 (a) Information for this answer comes from Section 21.3 in H&S. Points to include in your answer:

- relationship between x , y , z axes and positions of 6 L in octahedral $[\text{ML}_6]^{n+}$;
- crystal field theory assumes point charges;
- metal orbitals that point directly at ligands are d_{z^2} and $d_{x^2-y^2}$;
- repulsions between electrons in d_{z^2} and $d_{x^2-y^2}$ orbitals and ligand electrons greater than between electrons in d_{xz} , d_{xy} and d_{yz} orbitals and ligand electrons;
- include a sketch of Figure 21.2 in H&S;
- energies of d_{z^2} and $d_{x^2-y^2}$ orbitals raised with respect to barycentre, and energies of d_{xz} , d_{xy} and d_{yz} orbitals lowered.

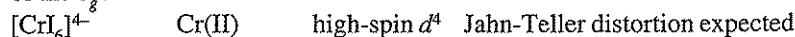
(b) First, note that each complex in the question contains Fe. To determine the ordering, consider the oxidation state of the Fe centre, and the field strength of the ligands: CN^- is a much stronger field ligand than H_2O ; Δ_{oct} is largest for combination of strong field ligand and higher oxidation state, and smallest for weaker field ligand and lower oxidation state. Order is:

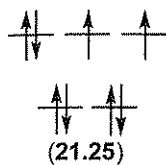


(21.24)

(c) Tetrahedral d^8 has configuration $e^4 t_2^4$ (21.24). For an electron to have orbital angular momentum contribution, it must be possible to transform the orbital it occupies into an equivalent, degenerate orbital by rotation – the three t_2 orbitals can be interconverted by rotations through 90° ; if all the t_2 orbitals in the tetrahedral complex are either singly or doubly occupied (i.e. t_2^3 or t_2^6), an electron cannot be transferred from one of the t_2 orbitals to another. In the tetrahedral d^8 ion, there is one fully and two singly-occupied t_2 orbitals and so there is an orbital contribution to the magnetic moment. Refer to Section 21.9 in H&S for greater detail.

21.36 (a) The complexes in the question are all octahedral. Jahn-Teller distortions are observed for d^9 and high-spin d^4 configurations where there is asymmetric filling of the e_g level:





$[\text{Cr}(\text{CN})_6]^{4-}$	Cr(II)	low-spin d^4	no Jahn-Teller distortion expected
$[\text{CoF}_6]^{3-}$	Co(III)	high-spin d^6	no Jahn-Teller distortion expected
$[\text{Mn}(\text{ox})_3]^{3-}$	Mn(III)	high-spin d^4	Jahn-Teller distortion expected

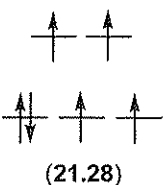
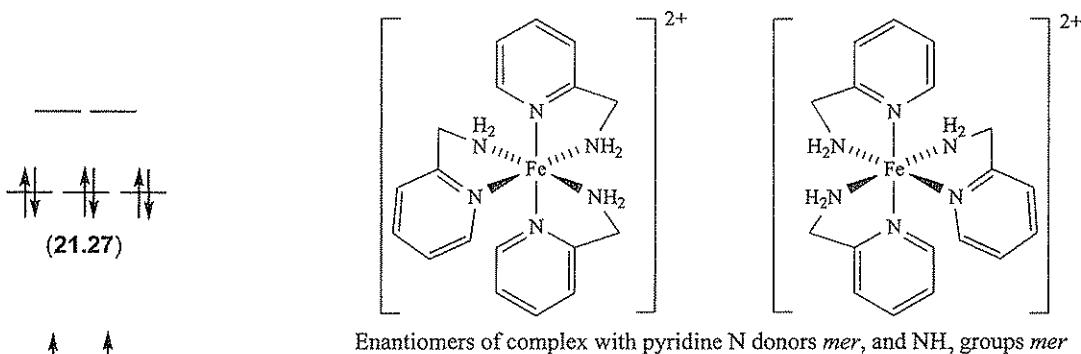
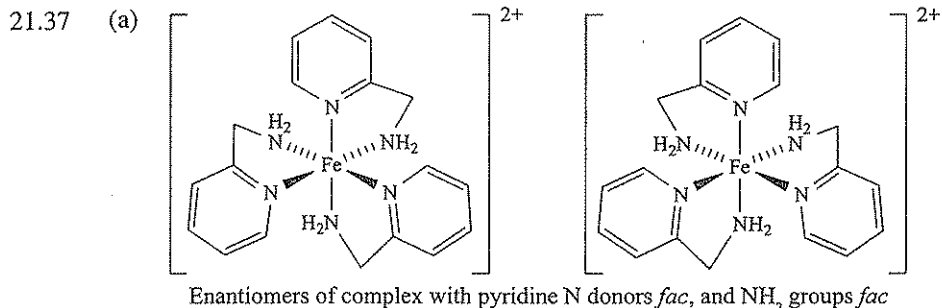
(b) In $[\text{Et}_4\text{N}]_2[\text{NiBr}_4]$ and $\text{K}_2[\text{PdBr}_4]$, complex ions are $[\text{NiBr}_4]^{2-}$ and $[\text{PdBr}_4]^{2-}$:

$[\text{NiBr}_4]^{2-}$	Ni(II)	d^8
$[\text{PdBr}_4]^{2-}$	Pd(II)	d^8

Two possible geometries: tetrahedral and square planar. The splitting of *d* orbitals and electronic configuration depends on the arrangement of the ligands. Splitting diagrams and orbital occupancies for tetrahedral and square planar d^8 configurations are shown in 21.25 and 21.26, respectively. If $[\text{NiBr}_4]^{2-}$ is paramagnetic, then it must have a tetrahedral structure. Since $[\text{PdBr}_4]^{2-}$ is diamagnetic, it is square planar.

(c) Information for this answer is in Section 21.4 in H&S. Points to include:

- valence orbitals of Ni are $3d$, $4s$ and $4p$;
- each ligand provides one orbital (consider as outward pointing hybrid of NH_3 that contains the lone pair);
- assume O_h symmetry for the complex;
- in O_h point group, metal s orbital has a_{1g} symmetry, p orbitals are degenerate with t_{1u} symmetry, d orbitals split into two sets, e_g (d_{z^2} and $d_{x^2-y^2}$) and t_{2g} (d_{xy} , d_{yz} , d_{xz});
- in O_h point group, 6 LGOs for the L_6 -fragment have a_{1g} , t_{1u} and e_g symmetries (see Figures 5.27 and 21.12 in H&S);
- by matching symmetries, form 6 bonding MOs (a_{1g} , t_{1u} and e_g), 6 antibonding MOs (a_{1g}^* , t_{1u}^* and e_g^*) and 3 non-bonding MOs (t_{2g});
- effectively, the d orbitals of Ni split into two levels, lower energy t_{2g} and higher energy e_g^* .



(b) Complex contains Fe(II), d^6 ; for octahedral complex, low-spin d^6 is diamagnetic (21.27) and high-spin is paramagnetic (21.28). At 120 K, the compound undergoes a change from low to high-spin; specifying a single temperature rather than a range implies that the change is abrupt rather than gradual (see Figure 21.28 in H&S).